Critical Adsorption in the Weak Surface Field Limit

J.-H. J. Cho and B. M. Law

Condensed Matter Laboratory, Department of Physics, Kansas State University, Manhattan, Kansas 66506-2601

(Received 9 October 2000)

We study critical adsorption in the small surface field (h_1) limit using a homologous series of critical liquid mixtures. The experiment data, in the one-phase regime, is accurately described by a universal surface scaling function $G_+(z/\xi_+, z/l_h)$ at distance z from the interface with correlation length ξ_+ and surface field length $l_h \sim |h_1|^{-\nu/\Delta_1}$, where $h_1 \sim \Delta\sigma$, the surface energy difference between the two components.

DOI: 10.1103/PhysRevLett.86.2070 PACS numbers: 68.03.Cd, 64.60.Fr

An understanding of surface phenomena at the interfaces of finite and semi-infinite critical systems has proven to be a particularly challenging problem. At these interfaces, the critical behavior is characterized not only by universal *scalar quantities* (such as the critical exponents) but also by *universal* surface functions which are *functions* of a number of dimensionless scaling variables. The existence of these scaling functions and scaling variables was predicted more than twenty years ago [1]; however, it has been only in the past couple of years that a number of these functions have been definitively determined experimentally and shown not only to be universal but also to scale the accordance with the predicted scaling variables [2–4]. In this paper, we are interested in the critical adsorption scaling function which describes the local variation in the composition at, for example, the noncritical liquid/vapor interface of a critical AB liquid mixture. This universal surface scaling function has been studied primarily in the limit of *strong adsorption* [4] where one component, say A, completely saturates the surface and the local volume fraction of the adsorbed component, $v(z)$, is a function of the dimensionless variable z/ξ, where z is the distance away from the noncritical interface at $z = 0$, and ξ is the correlation length. Competitive or *weak adsorption,* where the two components, A and B, possess similar surface energies, may be important in many situations, but has been little studied with the exception of [5]. For this case, the surface scaling function now depends not only upon z/ξ but also upon the surface field h_1, which determines the relative composition of the first monolayer immediately adjacent to the noncritical interface. In this paper, we quantitatively study weak adsorption at the liquid/vapor interface of critical mixtures; this subject should be of general interest for critical pure fluids, binary alloys, and ferromagnetic systems where analogous surface behavior is expected to occur [6].

At the noncritical liquid/vapor or liquid/solid interface of a critical AB mixture, the local volume fraction $v(z)$ of the adsorbed component is related to the local order parameter $m(z)$ via the scaling equation [1],

$$m(z) = v(z) - v_c\,, \tag{1}$$

$$= M\_t^{\beta} G_{\pm}(z/\xi_{\pm}, h_1 t^{-\Delta_1})\,, \tag{2}$$

where v_c is the critical volume fraction, and the universal surface scaling function $G_{\pm} \equiv G_{\pm}(x, y)$ is a function of two dimensionless variables: a dimensionless length $x = z/\xi_{\pm}$, where $\xi_{\pm} = \xi_{o\pm} t^{-\nu}$ is the bulk correlation length, and a dimensionless surface field variable $y = h_1 t^{-\Delta_1}$. For a critical mixture, the critical exponents β, ν, and Δ_1 take the values 0.328, 0.632, and 0.461, respectively, the reduced temperature $t = |T - T_c|/T_c$, while a + (−) subscript refers to a quantity in the one- (two-)phase region of the liquid mixture. In Eq. (2), M_t^{β} represents the bulk coexistence curve, therefore, in order that the local order parameter $m(z)$ reduces to the bulk order parameter at $z = \infty$, the surface scaling function $G_{\pm}(x \to \infty, y)$ must approach, respectively, 0 and 1 in the one- and two-phase regions. For strong adsorption, corresponding to $h_1 t^{-\Delta_1} \to \infty$, the first monolayer is completely saturated with the component possessing the lowest surface energy, and the function $G_{\pm}$ becomes independent of the precise value of h_1; hence, $G_{\pm}$ reduces to the simpler function,

$$P_{\pm} \equiv P_{\pm}(x) = G_{\pm}(x, \infty)\,. \tag{3}$$

Strong adsorption is expected to be extremely common in nature, and has been the subject of intensive study over the preceding twenty years. Definitive theoretical predictions for $P_{\pm}$ have become available only recently from surface renormalization group theory [7], Monte Carlo simulations [8], and local functional theory [9]. Experiments have also determined a universal form for $P_{\pm}$ which describes the results of four different ellipsometric experiments [4]; this form for $P_{\pm}$ agrees with an extensive neutron reflectometry study [10] but disagrees with the best theoretical estimates [8,9]. Corrections to scaling [11] may provide an explanation for this discrepancy between theory and experiment.

In our previous ellipsometric study of critical adsorption at the liquid/vapor interface [4], we ensured that we were in the strong adsorption limit by selecting critical liquid mixtures where the surface tension $\sigma_A \ll \sigma_B$; thus the liquid/vapor interface was completely saturated by component A. Such a study provides no information about the

 0031-9007/01/86(10)/2070(4)$15.00

surface field dependence exhibited in $G_{\pm}$ [Eq. (2)]; therefore it is of interest to study the weak adsorption regime, where $\sigma_A \approx \sigma_B$ and the h_1 field plays an important role. Innovative work by Desai, Peach, and Franck [5] provided the first experimental insights into this unusual adsorption regime, where saturation was observed for sufficiently large h_1, while the small h_1 behavior was qualitatively explained later in [12].

In this paper, we conduct a systematic study of the weak adsorption regime by studying a homologous series of critical AB liquid mixtures. Component B, corresponding to methyl formate (MF), is fixed, while component A is varied from undecane ($C11$) through to tetradecane ($C14$). The surface energy progressively increases from $C11$ to $C14$ as the chain length is increased. Hence, as we will see shortly, for this homologous series of mixtures, $C11$ and $C12$ possess a lower surface energy than MF with consequent n-alkane adsorption at the liquid/vapor surface; conversely, $C13$ and $C14$ possess a higher surface energy thus giving MF adsorption at the liquid/vapor interface. In terms of the surface field picture, there is a point between $C12$ and $C13$ where both components are adsorbed equally at the surface; this point, where $\sigma_A = \sigma_B$, corresponds to $h_1 = 0$. Therefore this study of a homologous series of critical liquid mixtures constitutes a study of critical adsorption in the weak surface field limit, where $h_1(\sim\sigma_A - \sigma_B)$ changes from a negative surface field (n-alkane adsorption) to a positive surface field (MF adsorption) as we progress from $C11$ through to $C14$. In this publication, only weak adsorption in the single phase regime of the liquid mixture is considered; the two-phase region, which is more difficult to analyze and interpret, will be considered in a later publication.

Ellipsometry is used to study the weak critical adsorption regime. In this technique, the ellipticity, $\overline{\rho} = \mathrm{Im}(r_p/r_s)$, is usually measured at the Brewster angle θ_B, where r_p (r_s) is the complex reflection amplitude parallel (perpendicular) to the plane of incidence. For thin films, relative to the wavelength of light $\lambda(= 632.8$ nm), the ellipticity $\overline{\rho}$ is related to an integral over the optical dielectric profile $\varepsilon(z)$ via the Drude equation [13]. To a good approximation, the Drude equation reduces to [14]

$$\overline{\rho} \approx -\frac{\pi}{\lambda}\frac{\sqrt{\varepsilon_1 + \varepsilon_2}}{\varepsilon_2}\int_0^{\infty}[\varepsilon(z) - \varepsilon_2]\,dz + \overline{\rho}_{\mathrm{BG}}(\xi_{\mathrm{nc}}), \tag{4}$$

for critical adsorption where this equation is expected to be valid for reduced temperatures $t \gtrsim 10^{-3}$ [15], and $\varepsilon_1(= 1)$ and ε_2 are, respectively, the air and liquid dielectric constants. The first term, in the region $z \geq 0$, corresponds to the contribution from critical adsorption, while the second term, $\overline{\rho}_{\mathrm{BG}}$, which is restricted to the region $z < 0$, originates from the variation in the *number density* of molecules on the *vapor side* of the interface. The term $\overline{\rho}_{\mathrm{BG}}$ is always *positive* [because $\varepsilon_1 < \varepsilon(z) < \varepsilon_2$ in the full Drude equation] where the magnitude is determined by a noncritical correlation length $\xi_{\mathrm{nc}} \sim 0.2$ nm [15]. For very thick films, $\xi \gtrsim \lambda$, Eq. (4) is no longer valid, and $\overline{\rho}$ can be obtained from a model for $\varepsilon(z)$ by numerically solving Maxwell's equations. The local volume fraction $\upsilon(z)$, and, hence, the surface scaling function $G_{\pm}$, can be related to $\varepsilon(z)$ using the two-component Clausius-Mossotti equation [16].

The ellipsometric critical adsorption data for the four liquid mixtures is shown in Fig. 1. These data possess all of the generic features expected in the region where the surface field h_1 is small and changes sign as a function of increasing chain length. Far from T_c at $t \sim 0.1$, where ξ is very small, $\overline{\rho}_{\mathrm{BG}}$ dominates the ellipticity $\overline{\rho}$; all four liquid mixtures possess very similar optical properties, hence, $\overline{\rho}_{\mathrm{BG}}$ is very similar for all mixtures. As $T \rightarrow T_c$, the critical adsorption contribution plays a more important role in Eq. (4); therefore $\overline{\rho}$ decreases *below* $\overline{\rho}_{\mathrm{BG}}$ for $\varepsilon(z) > \varepsilon_2$ and increases *above* $\overline{\rho}_{\mathrm{BG}}$ for $\varepsilon(z) < \varepsilon_2$. The optical dielectric constants for the n alkanes and for MF are, respectively, $\sim$2.0 and 1.78; the data in Fig. 1 indicate therefore that the n alkane preferentially adsorbs at the liquid/vapor surface for $C11$ and $C12$ while MF preferentially adsorbs at this interface for $C13$ and $C14$. Hence, the local volume fraction $\upsilon(z)$ in Eq. (1) corresponds to n alkane (MF) for $C11/C12$ ($C13/C14$). The change in the adsorption preferential (from n alkane to MF), which occurs between $C12$ and $C13$, implies that a zero in the adsorption preference, corresponding to $h_1 = 0$, occurs between these two liquid mixtures. At $h_1 = 0$, both A and B components adsorb equally at the liquid/vapor surface. The surface critical point is therefore *identical* to the bulk critical point, and we are in the vicinity of an "ordinary transition" [17,18], where $\upsilon(z) = \upsilon_c$ and therefore $\varepsilon(z) = \varepsilon_2$ for all $z \geq 0$ in Eq. (4), when $\overline{\rho} = \overline{\rho}_{\mathrm{BG}}$ for all t. The position where $h_1 = 0$ can be estimated by comparing the ellipticity at the peak $\overline{\rho}_{\mathrm{peak}}$ to $\overline{\rho}_{\mathrm{BG}}$. We expect that $\overline{\rho}_{\mathrm{peak}} = \overline{\rho}_{\mathrm{BG}}$

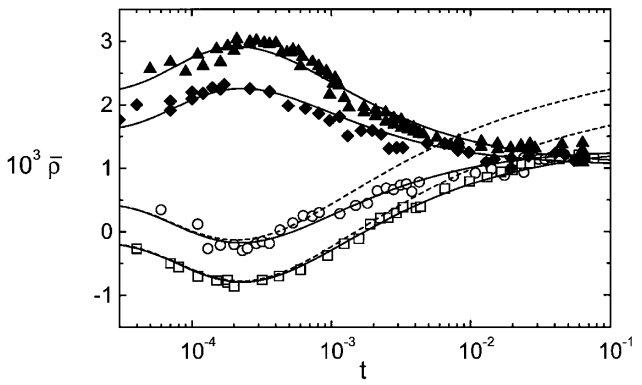

FIG. 1. Plot of the ellipticity $\overline{\rho}$ as a function of the reduced temperature t for the methyl formate + n-alkane homologous series of critical liquid mixtures, in the one-phase region. Experimental data: $C11$ (open squares), $C12$ (open circles), $C13$ (solid diamonds), and $C14$ (solid triangles). Model calculations: $\overline{\rho}_P$ (dashed lines) and $\overline{\rho}_G$ (solid lines)—see text for details.

at $h_1 = 0$; this occurs at an effective n-alkane mixture of $C12.6$ with critical temperature $T_c(C12.6) = 308.6$ K [19]. The surface field h_1 therefore increases as follows:

$$h_1(C11) < h_1(C12) < 0 < h_1(C13) < h_1(C14), \quad (5)$$

for this homologous series of liquid mixtures. A more precise definition for h_1 will be given below.

At sufficiently small t, the scaling variable $h_1 t^{-\Delta_1}$, exhibited in Eq. (2), will become sufficiently large so that G_+ crosses over to P_+ as indicated by Eq. (3). The $\overline{\rho}$ data should therefore be described by the P_+ function at sufficiently small t. In Fig. 1, we compare the mixtures $C11$ and $C12$ with $\overline{\rho}_P$ (dashed lines) calculated from P_+ [4]. Good agreement is found at sufficiently small t, as expected. $C12$ deviates more significantly away from $\overline{\rho}_P$ than $C11$; this is consistent with the identification that $|h_1(C11)| > |h_1(C12)|$. The other two liquid mixtures, $C13$ and $C14$, exhibit similar behavior [19].

Thus far, we have shown that this homologous series of critical liquid mixtures is consistent with a change in sign of the h_1 surface field which causes a change in preferential adsorption from n alkane for $C11$ and $C12$ to methyl formate for $C13$ and $C14$. To obtain a more definitive test of the experimental data, we must introduce a model for the universal surface scaling function $G_+(x, y)$, consistent with theoretical expectations, and test this model against experimental data. It is convenient to reexpress the scaling variable $y = h_1 t^{-\Delta_1}$ using an alternative dimensionless length scale,

$$Y = x|y|^{\nu/\Delta_1} = z/l_h, \quad (6)$$

where

$$l_h = \xi_{o+}|h_1|^{-\nu/\Delta_1} \quad (7)$$

is a new length associated with the h_1 field. For $z \gg l_h$, $G_+(x, Y) \rightarrow P_+(x)$, consistent with Eq. (3); while, for $z \ll l_h$, significant deviations from P_+ occur where [17]

$$m(z \ll l_h) \sim |h_1| z^{\kappa}, \kappa = (\Delta_1 - \beta)/\nu \approx 0.21. \quad (8)$$

The following ansatz,

$$G_+(x, Y) = P_+(x)[(1 + Y)/Y]^{-\Delta_1/\nu}, \quad (9)$$

correctly incorporates the asymptotic behavior exhibited in Eqs. (3) and (8), provided that one recalls that $P_+(x) \sim x^{-\beta/\nu}$ for small $x = z/\xi$ [1] and $Y \sim z$. The simple crossover form, given in Eq. (9), is expected to provide a reasonable representation of $G_+(x, Y)$ against which to test the experiment; a similar crossover ansatz, between appropriate asymptotic forms for P_+, provided a good description of critical adsorption experiments in the strong adsorption limit [4,10,20]. Before comparing Eq. (9) with the experiment, we first provide a physical interpretation for the surface field h_1. The most probable interpretation of h_1 is that it is proportional to the difference in surface energies, $\sigma_A - \sigma_{\mathrm{MF}}$, between the n alkane and MF in the mixture, namely,

$$h_1 \approx \frac{(\sigma_A - \sigma_{\mathrm{MF}}) l_\sigma^2}{k_B T_c}. \quad (10)$$

The strength of the surface field h_1 is determined by the relative adsorption energy $(\sigma_A - \sigma_{\mathrm{MF}}) l_\sigma^2$, compared with the thermal energy, $k_B T_c$, where l_σ is another noncritical length scale at the liquid/vapor interface. The sign of h_1 determines whether $\upsilon(z)$ represents the local volume fraction of n alkane or MF; if h_1 is negative (positive), then n alkane (MF) preferentially adsorbs at the interface and $\upsilon(z)$ corresponds to the local volume fraction of n alkane (MF).

Equations (1), (2), (6), and (9), applicable in the region $z \geq 0$, provide a model for critical adsorption which is expected to be valid for *all* values of the surface field h_1 [21]. In this model, $\upsilon(z)$ represents the local volume fraction of the preferentially adsorbed component. The local dielectric profile $\varepsilon(z)$ is derived from $\upsilon(z)$ using the two-component Clausius-Mossotti equation [16], while on the vapor side of the interface ($z < 0$), $\varepsilon(z)$ is supplemented by a model for the variation in the local *number density* (from liquid to vapor) controlled by the noncritical correlation length ξ_{nc} [15] [which gives rise to the background term $\overline{\rho}_{\mathrm{BG}}$ in Eq. (4)]. The ellipticity (denoted $\overline{\rho}_G$) for this model dielectric profile $\varepsilon(z)$ is determined by numerically solving Maxwell's equations. Many parameters control the magnitude and shape of $\overline{\rho}_G$ as a function of reduced temperature t. The mixture dependent parameters M_-, υ_c, and T_c were measured and fixed at their experimental values, while the critical exponents β, ν, and Δ_1 were fixed at the theoretical values listed above. This leaves three length scales, ξ_{o+}, l_h, and ξ_{nc}, which influence the behavior of $\overline{\rho}_G$ in different ways. The correlation length amplitude ξ_{o+} was measured in an independent turbidity experiment but varied within experimental error bars (which were rather large, $\sim$10%) in order to minimize chi squared, $\chi^2 = \Sigma_i(\overline{\rho}_i - \overline{\rho}_{Gi})^2/(N - 3)$, for each individual mixture. Here, $\overline{\rho}_i$ represents the experimental ellipticity for data point i, N is the total number of data points, and the number of adjustable parameters is three. In the strong adsorption limit ($h_1 t^{-\Delta_1}$ large) it has been shown that ξ_{o+} determines the reduced temperature t at which the peak in $\overline{\rho}$ occurs [15]. It is perhaps not surprising that this continues to hold true here because, although h_1 is small, $h_1 t^{-\Delta_1}$ continues to be large in the vicinity of the peak in $\overline{\rho}$ where the experimental data is well described by a model based solely upon P_+ (Fig. 1, dashed line) as mentioned above. The noncritical correlation length ξ_{nc}, as discussed in [15], determines the magnitude of $\overline{\rho}_{\mathrm{BG}}$; any variation in ξ_{nc} moves the whole $\overline{\rho}_G$ curve vertically by a *constant* amount without changing its shape. Hence, the shape difference between $\overline{\rho}_G$ and $\overline{\rho}_P$ generated by G_+ and P_+, respectively, is controlled purely by the length scale l_h. We have therefore minimized χ^2 by (i) adjusting ξ_{o+}, within errors bars, to correctly account for the reduced temperature t at which the peak in $\overline{\rho}$ occurs,

(ii) adjusting ξ_{nc} to describe $\overline{\rho}_{BG}$, and (iii) adjusting l_h to describe the crossover between $\overline{\rho}_{BG}$ and the peak position. The best $\overline{\rho}_G$ model is shown as a solid line in Fig. 1. The good agreement between $\overline{\rho}_G$ and experimental data indicates that the model contained within Eqs. (1), (2), (6), and (9) provides a good description of these experiments in the small h_1 field limit.

As a further test of the theory, according to Eqs. (7) and (10), we expect that $\Omega = (l_h/\xi_{o+})^{-\Delta_1/\nu}$ should be proportional to $\Sigma = |(\sigma_A - \sigma_{MF})/k_B T_c|$ with a slope l_σ^2, assuming that the length scale l_σ is similar for all members of this homologous series of critical liquid mixtures. It is difficult to measure the difference between the surface energies σ_A and σ_{MF} *within* the critical liquid mixtures. As an estimate of these energies, we have used the *pure* liquid/vapor surface tensions, where the methyl formate surface tension, including its variation as a function of temperature, has been shifted vertically upwards by a constant amount of $\sim 2 \mathrm{erg/cm}^2$ in order that $h_1 = 0$ for $C12.6$ at a critical temperature of $T_c(C12.6) = 308.6$ K [19]. In Fig. 2, we have plotted Ω as a function of Σ; the solid line, which has been constrained to pass through the origin, is the best fit to the experimental data from which we obtain $l_\sigma = 0.57$ nm. As expected, l_σ is of order a molecular size; its value will depend upon the particular liquid mixture (or homologous series of liquid mixtures) that is under consideration.

In summary, we have studied critical adsorption at the liquid/vapor surface of a homologous series of critical liquid mixtures, specifically methyl formate + n alkane. As the n alkane is increased from undecane to tetradecane, the preferentially adsorbed component at this surface changes from n alkane to methyl formate. This series of critical liquid mixtures is therefore in the weak adsorption limit, where the surface field h_1 is small and changes sign with increasing alkane chain length. In this weak field regime, a reasonable ansatz for the surface scaling function $G_+(z/\xi_+, z/l_h)$, which possesses the predicted asymptotic behavior, is provided in Eq. (9). The experimental ellipticity data, which deviates markedly from the strong critical adsorption regime (Fig. 1, dashed lines), is well described by Eq. (9) using a single l_h for each liquid mixture (Fig. 1, solid lines). As predicted, we also find that $l_h \sim |\Delta\sigma|^{-\nu/\Delta_1}$ (Fig. 2), where $\Delta\sigma = \sigma_A - \sigma_{MF}$ is the surface tension difference between the n-alkane and methyl formate components.

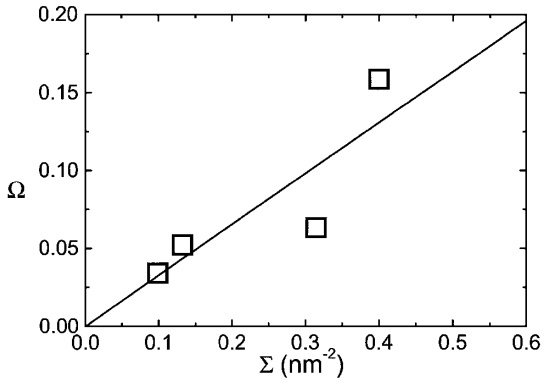

FIG. 2. Plot of $\Omega = (l_h/\xi_{o+})^{-\Delta_1/\nu}$ against $\Sigma = |\sigma_A - \sigma_{MF}|/k_B T_c$, where, according to Eqs. (7) and (10), the slope is equal to l_σ^2. The solid line is the best fit line through the data, which has been constrained to pass through the origin.

Acknowledgment is made to the donors of the Petroleum Research Fund, administered by the American Chemical Society, and to the National Science Foundation through Grant No. DMR-9631133 for partial support of this research.

[1] M. E. Fisher and P.-G. de Gennes, C. R. Seances Acad. Sci. Ser. B **287**, 207 (1978).
[2] A. Mukhopadhyay and B. M. Law, Phys. Rev. Lett. **83**, 772 (1999).
[3] R. Garcia and M. H. W. Chan, Phys. Rev. Lett. **83**, 1187 (1999).
[4] J. H. Carpenter *et al.,* Phys. Rev. E **59**, 5655 (1999); **61**, 532 (2000).
[5] N. S. Desai, S. Peach, and C. Franck, Phys. Rev. E **52**, 4129 (1995).
[6] H. W. Diehl, Int. J. Mod. Phys. B **11**, 3503 (1997).
[7] H. W. Diehl and M. Smock, Phys. Rev. B **47**, 5841 (1993); **48**, 6470(E) (1993).
[8] M. Smock, H. W. Diehl, and D. P. Landau, Ber. Bunsen-Ges. Phys. Chem. **98**, 486 (1994).
[9] Z. Borjan and P. J. Upton (to be published).
[10] J. Jestin, G. Zalczer, and L. T. Lee (to be published).
[11] S. B. Kiselev, J. Chem. Phys. **112**, 3370 (2000).
[12] A. Ciach, A. Maciolek, and J. Stecki, J. Chem. Phys. **108**, 5913 (1998).
[13] P. K. L. Drude, *The Theory of Optics* (Dover, New York, 1959), p. 292.
[14] Equation (4) is obtained from the Drude equation using the approximation that $|\varepsilon(z) - \varepsilon_2| \ll \varepsilon_2 - \varepsilon_1$ in the region $z \geq 0$.
[15] D. S. P. Smith and B. M. Law, Phys. Rev. E **52**, 580 (1995); **54**, 2727 (1996); D. S. P. Smith, B. M. Law, M. Smock, and D. P. Landau, *ibid.* **55**, 620 (1997).
[16] If $v(z)$ represents the local volume fraction of A, then $\varepsilon(z)$ is related to $v(z)$ via the two-component Clausius-Mossotti relation, $f[\varepsilon(z)] = v(z)f(\varepsilon_A) + [1 - v(z)]f(\varepsilon_B)$, where $f(x) = (x - 1)/(x + 2)$.
[17] U. Ritschel and P. Czerner, Phys. Rev. Lett. **77**, 3645 (1996).
[18] Note that, as discussed in [17], the "surface enhancement parameter" c_0 (which determines whether a surface transition is ordinary, special, or extraordinary) is a dangerous irrelevant variable; therefore, in the limit of small actual surface field $\mathbf{h}_1$ and large $c_0 \gg 0$ (near an ordinary transition), the "effective" surface field (used throughout this paper) $h_1 = \mathbf{h}_1/c_0^y$, where y is an exponent.
[19] J.-H. J. Cho and B. M. Law (to be published).
[20] A. J. Liu and M. E. Fisher, Phys. Rev. A **40**, 7202 (1989).
[21] In Eq. (9), the "P3a model" from [4] has been used for $P_+(x)$.